Density functional theory study of adsorption of H2O, H, O, and OH on stepped platinum surfaces

Manuel J. Kolb, Federico Calle-Vallejo, Ludo B. F. Juurlink, and Marc T. M. Koper

---

Articles you may be interested in

Enantioselectivity of (321) chiral noble metal surfaces: A density functional theory study of lactate adsorption
J. Chem. Phys. **139**, 224709 (2013); 10.1063/1.4839755

Adsorption of lactic acid on chiral Pt surfaces—A density functional theory study
J. Chem. Phys. **138**, 084705 (2013); 10.1063/1.4792441

Hydrogen fluoride adsorption and reaction on the α-Al2O3(0001) surface: A density functional theory study
J. Chem. Phys. **136**, 114701 (2012); 10.1063/1.3694102

Lifting the Pt{100} surface reconstruction through oxygen adsorption: A density functional theory analysis
J. Chem. Phys. **122**, 184709 (2005); 10.1063/1.1893718

A density functional theory study of the adsorption of sulfur, mercapto, and methylthiolate on Au(111)
J. Chem. Phys. **116**, 784 (2002); 10.1063/1.1424292

Density functional theory study of adsorption of H₂O, H, O, and OH on stepped platinum surfaces

Manuel J. Kolb,[1] Federico Calle-Vallejo,[1,2] Ludo B. F. Juurlink,[1] and Marc T. M. Koper[1,a)]

[1]*Leiden Institute of Chemistry, Leiden University, PO Box 9502, 2300 RA Leiden, The Netherlands*
[2]*Laboratoire de Chimie, École Normale Supériéure de Lyon, 46 alle d'Italie, 69364 Lyon cedex 07, France*

We report on density functional theory (DFT)-GGA (generalized gradient approximation) computed adsorption energetics of water and the water-related fragments OH, O, and H on stepped Pt surfaces in the low coverage limit. The Pt(100) step edge as encountered on Pt(533) shows increased binding for all species studied, while the Pt(110) step edge, as found on Pt(553) shows only significantly enhanced binding for O and OH. Comparing these results to ultra high vacuum experiments reveals that DFT can explain the main experimental trends semiquantitatively. © *2014 AIP Publishing LLC.* [http://dx.doi.org/10.1063/1.4869749]

INTRODUCTION

Platinum plays a key role in catalysis, and it is ideally suited as electrocatalyst for low-temperature Polymer Electrolyte Membrane (PEM) fuel cells,[1] water electrolysis, and many other electrochemical reactions. Understanding the interaction between platinum surfaces and water molecules at the atomic level is important for the further improvement of its activity and in creating new, cost-effective catalysts that perform similarly to platinum.[2,3] In order to achieve a complete picture of real catalytic surfaces, which usually consist of small particles on a support, not only the consideration of high symmetry facets of the surface is required, but also the influence of step and kink sites on adsorption and reactivity.[4,5] The effect of isolated step sites can be systematically studied using regularly stepped surfaces. These consist of flat terraces of high symmetry facets interrupted by monatomic steps. This setup allows for direct observation of the influence of the step type on the reactivity, thereby providing some insight on the influence of steps on the overall catalytic activity. Traditionally, most experimental and theoretical studies devoted to the interaction of water with platinum surfaces have dealt with either flat Pt(111) surfaces or other facets with rather low surface indices.[6,7] While this helps to reduce computational efforts, such calculations give limited insight into the adsorption energies of isolated steps due to the influence of step-step interactions and the interactions between all terrace adsorption sites with the step edge on short terraces. However, more recent computational studies[8–10] have considered surfaces with steps of a separation distance similar to the one studied in this paper.

In previous experimental work from our group,[11] we studied the desorption of H, O, and H₂O from two stepped Pt surfaces, Pt(533) and Pt(553), using the Temperature Programmed Desorption (TPD) technique in ultra-high vacuum (UHV). The Pt(533) surface consists of a 4 atom long terrace of (111) character and a (100) step edge, whereas the Pt(553) surface has a 5 atom long (111) terrace and a (111) step edge. Side- and top-views of the surfaces are shown further into the paper as Figures 1 and 2.

It was found from TPD that hydrogen desorbs in a two-peak structure from Pt(533) and in a more complicated pattern with two or three peaks from Pt(553). Atomic oxygen was found to desorb in a two-peak structure from both surfaces. The high-temperature peak was found at higher temperatures for Pt(533) compared to Pt(553).[11] Desorption of H₂O was observed to exhibit a three-peak structure for both Pt(533) and Pt(553). The low-energy peak was assigned to multi-layer desorption. The high-energy peak was attributed to desorption from steps, since it was not observed on the flat Pt(111) surface. The intermediate-temperature peak was located at a temperature comparable to that of Pt(111), therefore it was assigned to desorption from terraces. The high-temperature peak was detected at comparable temperatures for both surfaces, suggesting that the adsorption energies of water for the two different step geometries are not significantly different. For most adsorbates, it was concluded that step sites should bind adsorbates stronger than terrace sites, and for H and O this tendency is stronger for the (100)-type step site. For a more detailed description of the desorption spectra, we refer to the original publication.

The aim of this study is to establish a qualitative explanation for the results of the TPD experiments, by computing the adsorption energy of water and its dissociation products H, O, and OH on the stepped surfaces Pt(533) and Pt(553) using Density Functional Theory (DFT). This will serve as a benchmark for future studies on the interaction of water with adsorbate-covered stepped Pt surfaces and complements other studies on the intrinsic different catalytic activities of (100) and (110) step edges.[12]

COMPUTATIONAL METHODS

The computations were performed using the *ab initio* density functional code VASP[13–16] using the PBE exchange-correlation functional[17] and PAW potentials.[18,19] The PBE

---

a)Author to whom correspondence should be addressed. Electronic mail: m.koper@chem.leidenuniv.nl
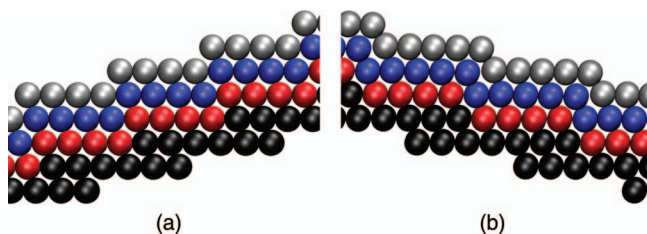
FIG. 1. Side view onto the two model surfaces, (a) Pt(533) and (b) Pt(553).

functional was chosen in order to obtain reasonable adsorption energies across the whole range of species studied here and to adequately describe hydrogen bonding among water molecules[20] for future calculations that include solvation. The k-point sampling was done using a Monkhorst-Pack scheme[21] using $9\times9\times1$ sampling for the Pt(111) surface and a $3\times9\times1$ sampling for the stepped Pt(533) and Pt(553) surfaces. A basis set with a cut-off energy of 550 eV was chosen. For all calculations, first order Methfessel-Paxton smearing with a sigma of 0.2 was applied and all energies were extrapolated to an electronic temperature of 0 K. All calculations were performed spin restricted. The replicated images of the cells due to the periodic boundary conditions were separated by about 20 Å of vacuum. Gas phase species were calculated using a $10\times10\times10$ Å unit cell with a $1\times1\times1$ k-point sampling in which the gas phase species were placed.

The Pt(111) surface was a 2×2 replicated surface unit cell with 3 relaxing layers at the top and 2 layers fixed at bulk positions at the bottom. This is beyond what is necessary for convergence on a (111) surface, but proved necessary to achieve consistency with the stepped surfaces. Figures 1(a) and 1(b) show a side view of the model stepped surfaces. Fixed layers are black, surface layers are silver, the first subsurface layer is blue, and the second subsurface layer is red. Note that when using a 4-layer model to stepped surfaces the atom that forms the lower step edge has a nearest neighbour that is fixed in its bulk position, resulting in a distorted step edge. This influences the total energy for that cell and the resulting step geometry. Therefore, we increased the number of layers to 5 to solve this problem. The resulting unit cell was then replicated in the direction parallel to the step

edge to achieve similar adsorbate-adsorbate separation as on Pt(111).

The free energies of adsorption of H, O, OH, and H_2O were calculated as follows:

$$\Delta G_{ads,H} = G_{total,H_{ads}} - G_{clean} - \frac{1}{2}G_{H_2(g)}, \qquad (1)$$

$$\Delta G_{ads,O}^{O_2(g)} = G_{total,O_{ads}} - G_{clean} - \frac{1}{2}G_{O_2(g)}, \qquad (2a)$$

where

$$G_{O_2(g)} = 2\big(G_{H_2O(g)} - G_{H_2} - \Delta G_{form,exp}^{H_2O}\big) \qquad (2b)$$

and

$$\Delta G_{form,exp}^{H_2O}(g) = -2.37 \text{ eV at } P = 1 \text{ atm and } T = 298.15 \text{ K}, \qquad (2c)$$

$$\Delta G_{ads,O}^{H_2O} = G_{total,O_{ads}} - G_{clean} - G_{H_2O}(g) + G_{H_2(g)}, \qquad (3)$$

$$\Delta G_{ads,OH} = G_{total,OH_{ads}} - G_{clean} - G_{H_2O}(g) + \frac{1}{2}G_{H_2(g)}, \qquad (4)$$

$$\Delta G_{ads,H_2O} = G_{total,H_2O_{ads}} - G_{clean} - G_{H_2O(g)}. \qquad (5)$$

Each individual G was calculated as follows:

$$G_{A_{ads}} = E_{DFT,A} + ZPE(A) - T*S(A)_{vib} \qquad (6)$$

for adsorbate A and

$$G_{B(g)} = E_{DFT,B} + ZPE(B) - T*S(B) \qquad (7)$$

for gas-phase species B. Note that S(B) is the total entropy and is taken from reference tables for gas phase species.[22]

The free energies of adsorption of oxygen were calculated for two references (Eqs. (2a) and (3)). One for comparison to gas phase O_2 (Eq. (2a)) which is the more relevant reference for comparison to TPD experiments, that is calculated based on the experimental formation energy of water (Eq. (2b)), in order to avoid the inaccuracy of the DFT value for O_2.[23,24] The other reference is calculated using water as a reference (Eq. (3)), which is the relevant reference value for comparison to electrochemistry and for the possible formation of OH on step edges. All adsorption energies below are Gibbs energies and corrected for zero-point energy (ZPE) and
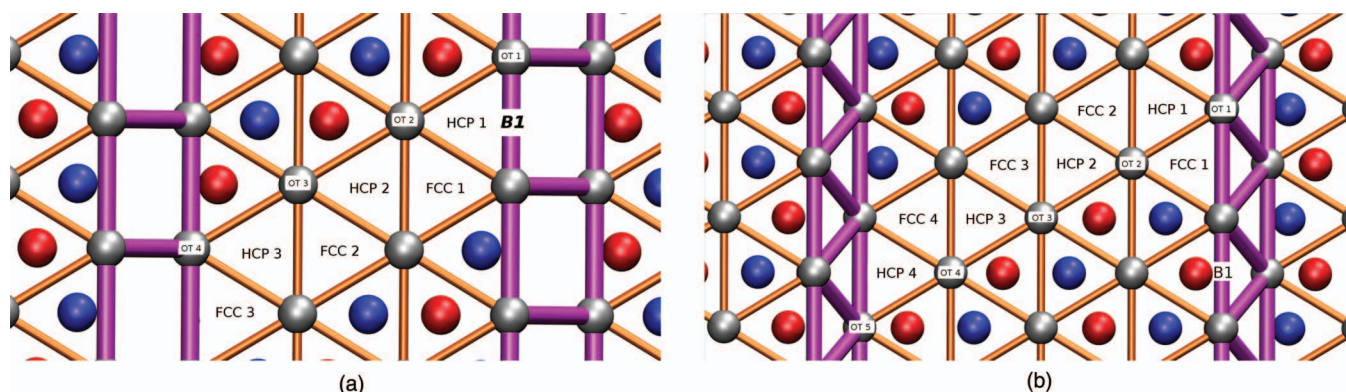

FIG. 2. Adsorption sites on the stepped surfaces (surface layer atoms marked silver, second layer atoms blue, and third layer atoms red), (a) Pt(533) and (b) Pt(553).

vibrational entropy at 298 K, following the methods described by Loffreda.[25]

The adsorption sites on Pt(533) and Pt(553) surfaces are illustrated in Figures 2(a) and 2(b). Platinum atoms in the surface layer are colored in silver, those in the subsurface layer are blue, and those in the second layer below the surface are red. The adsorption sites are OT for on-top adsorption, B for bridge sites, and FCC/HCP for the two threefold hollow adsorption sites. Bronze bonds represent the direct connection between two surface atoms in the (111) plane, magenta bonds show direct connections in the (100)/(110) steps. A full catalogue of adsorption sites, their associated energies, vibrational frequencies, and geometry information is available in the supplementary material.[26]

RESULTS AND DISCUSSION

The Pt(533) and Pt(553) surfaces

In the absence of adsorbates, the surface relaxation is not extensive, i.e., the displacements of edge atoms are quite small. The total energy gained from relaxing the top three layers of the surface is small (0.0122 and 0.0076 eV per platinum atom in the unit cell for Pt(533) and Pt(553), respectively). In both optimized structures, the exposed surface area is minimized by retracting the edge atoms into the deeper layers, as can be seen in Figures 1(a) and 1(b). These relaxation effects on edge atoms lead to a slight tilt of the (111) surface towards the (533)/(553) surface normal.

Adsorption energies on the stepped surfaces are not completely converged with respect to the thickness of the slab. However, tests showed that this leads to a uniform shift of the adsorption energies of all sites. The results of these tests can be found in the supplementary material.[26] This allows us to look primarily at general trends in adsorption energies. We emphasize that the simultaneous full convergence of all adsorption energies for all species on all surfaces considered here is not within the scope of this paper. In order to observe possible trends in the shift of the d-band center for the step edge atoms, the LDOS (local density of states) for the surface atoms of the Pt(111) facet and step edge atoms of the two studied surfaces were calculated and can be found in the supplementary material.[26] No obvious shift or difference in the d-band center for either surface was observed.

Hydrogen adsorption

The distinct adsorption sites for hydrogen are the on-top position, the bridge position between two surface platinum atoms and the two threefold hollow sites, HCP and FCC. These adsorption sites are, from an energetic point of view, almost equivalent, with a slight preference towards the threefold hollow sites. The results for Pt(111) using our approach can be found in Table I. Earlier results obtained by Olsen *et al.*[27] with two different generalized gradient approximation (GGA) functionals (BP and PW91) revealed a similar range of adsorption energies as computed here. The functionals in those studies however showed a clear trend towards on-top adsorption, which is not found here. It should be noted that

TABLE I. Adsorption energies for hydrogen on Pt(111), Pt(533), and Pt(553).

Adsorption site	$G_{Pt(111),H_{ad}}$ [eV]	$G_{Pt(533),H_{ad}}$ [eV][a]	$G_{Pt(553),H_{ad}}$ [eV][a]
OT terrace (OT2/OT3)	−0.26	−0.20	−0.18
HCP terrace (HCP2/HCP3)	−0.26	−0.18	−0.15
FCC terrace (FCC2/FCC3)	−0.29	−0.21	−0.21
Bridge terrace	−0.25	…	…
Bridge B1	…	−0.41	−0.26
On-top OT1	…	−0.26	−0.19
FCC1	…	−0.19	−0.28
HCP1	…	−0.23[b]	−0.28
On-top OT4/OT5	…	−0.27	−0.16

[a] Adsorption energy converged to 0.05 eV for present layer thickness (see the supplementary material[26]).
[b] Approximate energy, atom fixed at unstable adsorption site.

the results of Olsen *et al.*[27] did not take ZPE and vibrational entropy into account, so they cannot be directly compared to the Gibbs energies of adsorption computed here.

For the stepped surfaces, almost all bridge sites on the terrace do not contribute to adsorption, because the two neighbouring threefold hollow sites are, unlike on the flat Pt(111) surface, no longer equivalent in energy. This leads to an energy gradient that moves the hydrogen atom out of the bridge position towards the neighbouring site with the strongest binding. In Table I, we only provide the adsorption sites in the middle of the terrace for comparison to pristine Pt(111). A full overview of all adsorption sites can be found in the supplementary material.[26]

On the Pt(533) surface, the strongest binding site is the B1 site on the step edge. The OT1 site, which is also located on the step edge, shows enhanced binding compared to the OT site on the terrace as well. However, the nearby B1 site is significantly more stable, therefore on real surfaces the OT1 site will probably not play a role. Another binding site is the OT4, which is located on the lower step edge and also shows slightly enhanced binding compared to Pt(111). It should be noted that this site has a twofold coordination, despite being identified as an on-top site, since it is also located close to the platinum atom in the upper step edge. The threefold hollow sites on the step edge, named FCC1 and HCP1, show binding energies comparable to the FCC1 site on the Pt(533) terrace, although the HCP1 site is no longer stable and hydrogen will move to the B1 site with no noticeable barrier. To estimate the energy of this binding site, the atom was fixed at the HCP1 site, which then showed slightly enhanced binding compared to the terrace, even in this unrelaxed HCP position.

On the Pt(553) surface, the situation is significantly different. The most important sites on the surface are again shown in Table I. We found that B1 on the step edge of this surface binds hydrogen significantly weaker than the same site on the Pt(533) step edge. The B1 site is therefore no longer the strongest binding site, but is energetically comparable to the FCC1 position. The lower step edge on Pt(553) also binds hydrogen significantly weaker than the comparable geometry on Pt(533). The terrace sites, however, show very similar binding energies as the Pt(533) terraces. This means

that the most important difference between the Pt(553) and the Pt(533) surfaces is the stronger stabilization provided by the Pt(533) step edge.

Comparison to experiment

In the temperature-programmed desorption experiments of van der Niet *et al.*,[11] desorption of deuterium was compared on Pt(111), Pt(533), and Pt(553). They found that the introduction of steps only leads to stabilization of H on the Pt(533) step edge and not on Pt(553). Our DFT findings are in good agreement with those results. Reproducing the details of the TPD spectra requires a more detailed account of lateral interactions and surface diffusion, as presented in Refs. 28 and 29.

Oxygen adsorption

In order to ensure consistency with previous results (e.g., Ref. 30), we will briefly discuss the results for oxygen adsorption on Pt(111). We find that the FCC site is the most stable, with an adsorption energy of -1.14 eV with respect to the $O_2(g)$ reference or 1.23 eV on the H_2O-based scale. This is followed by the HCP site and the on-top site. The bridge position is, in contrast to hydrogen, unstable and leads to a shift into one of the hollow sites. It should be noted that our results are all obtained using non-spin-polarized calculations, leading to a slightly underestimated binding for the on-top site, as can be expected due to an increased net spin of the bonded oxygen when performing spin polarized calculations.[31] We find an energy difference between spin restricted and unrestricted calculations of about 0.1 eV for the on-top site, while no changes are observed for any site with an oxygen atom that is coordinated to more than one platinum atom. None of the affected sites plays a role in the actual adsorption since even their corrected adsorption energies are well above all neighbouring sites. On the stepped Pt(533) surface, the situation is similar to the case of hydrogen discussed earlier. The binding energies for the most important sites can be found in Table II. The B1 site again shows enhanced binding compared to the Pt(111) surface, although we find no stable binding site on the lower step edge as we did for hydrogen. The FCC1 site on the upper step edge shows an adsorption energy that is comparable to the FCC site on the Pt(111) surface. On the Pt(553)

TABLE II. Adsorption energies for oxygen on Pt(111), Pt(533), and Pt(553).

Adsorption site	$G_{O_{ad},Pt(111)}$ [eV][a]	$G_{O_{ad},Pt(533)}$ [eV][a,b]	$G_{O_{ad},Pt(553)}$ [eV][a,b]
On-top, terrace	0.14/2.51	0.42/2.79	0.43/2.79
HCP hollow, terrace	$-0.68/1.69$	$-0.62/1.75$	$-0.57/1.80$
FCC hollow, terrace	$-1.14/1.23$	$-0.96/1.41$	$-0.92/1.45$
Bridge B1	...	$-1.43/0.94$	$-1.10/1.27$
FCC1	...	$-1.07/1.30$	$-1.29/1.08$
OT5	...	...	$-0.91/1.46$

[a]First value for $O_2(g)$ reference, second for H_2O reference.
[b]Adsorption energy converged to within 0.05 eV for present layer thickness (see the supplementary material[26]).

surface, the results are again notably different. The strongest adsorption site is now the FCC1 site on the upper step edge, comparable to the case for hydrogen. Additionally, the OT5 site, which actually has threefold coordination due to its position on the lower edge of the step, is able to bind oxygen.

In conclusion, our calculations for oxygen adsorption on stepped platinum surfaces show that the strongest binding would occur at the B1 position on Pt(533), which binds oxygen significantly stronger than on Pt(111). On Pt(553) we find an increased binding compared to Pt(111) but this increase is less than on Pt(533).

Comparison to experiment

Van der Niet *et al.*[11] found in their TPD study that oxygen desorbing from Pt(533) shows a two-peak structure with a peak at 774 K and another one at 663 K. The low-temperature peak was found at a comparable temperature as desorption from Pt(111) and was, therefore, assigned to desorption from terraces. The high-temperature peak was assigned to oxygen desorption from steps. On Pt(553) they found a similar two-peak structure, however the high-energy peak was located at the somewhat lower temperature of 738 K. This suggests that the step edge in Pt(533) binds oxygen stronger than Pt(111) terraces and also stronger than the Pt(553) step edge. This matches satisfactorily our DFT results. The change of the preferred adsorption site from the B1 site on the step edge for Pt(533) to the FCC1 site behind the step edge is in agreement with the results observed by DFT(LDA) and STM in the study by Feibelman *et al.*[32]

H₂O adsorption

For Pt(111), we find an adsorption energy for water monomers adsorbed in a flat on-top position of 0.28 eV. This value differs significantly from earlier studies, none of which included both ZPE and vibrational entropy. Our raw DFT energy E, -0.23 eV is closer to the literature results of -0.30 eV calculated with PW91.[33,34] The Gibbs energy of water adsorption is rather sensitive to the actual observed geometry of adsorption. The actual value for vibrational entropy changes by as much as 30% when rotating the water molecule at a certain site. Nevertheless, this only changes the adsorption energy by about 0.05 eV at most, and therefore the general trends detailed here are still expected to be valid. For the sake of consistency, in the following we will continue using the same convention as before and provide the Gibbs energies of adsorption at 298 K. Due to this convention most adsorption energies will be positive, which is intuitively expected, because water will have desorbed from the surface long before reaching that temperature.[11] We also note that for water the convergence with regard to the number of layers is faster than for oxygen and hydrogen.

The tendency of water to bind preferentially atop platinum atoms is still valid on the stepped surfaces. Table III contains the adsorption energies for the aforementioned Pt(111) surface and for both stepped surfaces. However, the on-top positions on the step edge bind water with a binding strength of 0.06 eV and 0.07 eV for the Pt(533) and Pt(553) sur-

TABLE III. Adsorption energies for H_2O on Pt(111), Pt(533), and Pt(553), most stable geometries at the given points.

Adsorption site	$G_{H_2O_{ad},Pt(111)}$ [eV]	$G_{H_2O_{ad},Pt(533)}$ [eV][a]	$G_{H_2O_{ad},Pt(553)}$ [eV][a]
On-top, terrace, flat	0.28	0.27	0.24
OT1, step edge	. . .	0.06	0.07

[a]Adsorption energy converged to within 0.05 eV for present layer thickness (see the supplementary material[26]).

face, respectively, compared to 0.28 eV for Pt(111). This is in qualitative agreement with earlier results for (100) and (110) step edges which showed an increase in binding energy E of ~0.15 eV for the step edge compared to flat Pt(111) surfaces.[9]

Comparison to experiment

In the TPD experiments performed by Van der Niet *et al.*,[11] it was found that water desorbs from stepped platinum surfaces in a three-peak structure. The highest temperature peak was always assigned to desorption from the step edges, since no comparable peak was observed on the Pt(111) surface. The desorption temperature for the step-related peak was found ~10 K lower on the Pt(533) surface compared to the Pt(553) surface. The intermediate-temperature peak was assigned to desorption from terraces, since it agrees with the peak observed on Pt(111). The lowest-temperature peak was assigned to the desorption of water from multi-layer water structures. The DFT results presented here show qualitative agreement with experiment in that the terrace adsorption energy is lower than the adsorption energy on the step edge. It should be noted that the difference in adsorption energies for Pt(533) and Pt(553) observed experimentally is not explained by the present calculations of the adsorption of single water molecules.

OH adsorption

As OH is an important water-related intermediate at electrochemical interfaces, we also provide adsorption energies for OH on the three surfaces. Pt(111) shows a large preference to adsorb the OH molecule in either an atop or a bridge position. The FCC and HCP hollows show significantly reduced binding energies. Adsorption energy values for OH on Pt(111) can be found in Table IV. Our values are in agreement with the results by Nørskov and Campbell *et al.*[35] for the Pt(111) surface, who reported an adsorption energy of −1.54 eV against a gas-phase OH reference. Using their formation energy for gas-phase OH of 0.32 eV and transforming it to our energy reference yields an adsorption energy of +1.12 eV for the OH adsorption on Pt(111). Our adsorption energy value with ZPE correction but without vibrational entropy for the isolated OH molecule on the Pt(111) surface is 0.91 eV, which is reasonably close given that different functionals were used.

Introducing steps into the surface breaks the symmetry of the adsorption sites in one direction of the surface. FCC and HCP hollow sites are not found to be local minima near

TABLE IV. Adsorption energies for OH on Pt(111), Pt(533), and Pt(553).

Adsorption site	$G_{OH_{ads},Pt(111)}$ [eV]	$G_{OH_{ad},Pt(533)}$ [eV][a]	$G_{OH_{ad},Pt(553)}$ [eV][a]
On-top, terrace, flat	1.02	1.16	1.18
Bridge, terrace (parallel)	1.02[b]	1.08	1.22
Bridge, terrace (other directions)	1.02[b]	1.23	1.16
Bridge B1	. . .	0.27	0.66
HCP hollow, terrace	1.54	Unstable	Unstable
FCC hollow, terrace	1.27	Unstable	1.44

[a] Adsorption energy converged to within 0.05 eV for present layer thickness (see the supplementary material[26]).
[b]No directional influence on the Pt(111) surface.

step edges, suggesting that on Pt(111) they were mainly stabilized into a meta-stable position by the symmetry of the surface. The Pt(533) surface shows an increased binding at the step-edge bridge site, similar as for the other adsorbates. Additionally, we found a difference in the adsorption energy for the terrace bridge sites depending on their orientation. Bridge sites at the terraces of Pt(533) parallel to the step edge were found to be no longer stable near the step edge, while all other bridge sites were stable, although they show decreased binding compared to Pt(111). The binding energy on the step edge of Pt(553) is significantly less favorable compared to the Pt(533) surface. The bridge sites on the Pt(553) terrace show no directional variance with respect to binding energy, and all of them are stable. In conclusion, OH prefers to bind to step edges in the B1 position on both surfaces and is ~0.7 eV more stable for Pt(533) and ~0.4 eV for Pt(553) compared to Pt(111).

Comparison to experiment

The adsorption of OH cannot be directly studied in UHV. Typically, the generation of OH_{ads} is performed by dosing water onto a Pt surface pre-covered with O_{ads}. This leads to the following net reaction:

$$H_2O_{ads} + O_{ads} \rightarrow 2OH_{ads}. \qquad (8)$$

Our calculations suggest that this reaction is exothermic on the Pt(100) step, endothermic on the Pt(111) surface, and almost thermoneutral for the step edge on Pt(553), with a ΔG of −0.49 eV at 298 K for the Pt(533) surface, +0.52 eV for Pt(111), and −0.01 eV for the Pt(553) surface (see Table V). These numbers were calculated by considering all adsorbates in isolation on their most stable adsorption sites. No interaction with water was considered, which is certainly important when studying electrochemical reactions.[36,37] From these results, we can conclude that reaction (8) generates

TABLE V. ΔG for reactions (8) and (9) on different surfaces at 298 K.

	$H_2O_{ads} + O_{ads} \rightarrow 2OH_{ads}$ (Reaction (8))	$H_2O_{ads} \rightarrow OH_{ads} + H_{ads}$ (Reaction (9))
Pt(111)	0.52	0.47
Pt(533)	−0.49	−0.23
Pt(553)	−0.01	0.33

more OH$_{ads}$ on the Pt(533) step compared to Pt(553). On Pt(111) this reaction should not take place if stabilizing effects are not accounted for. Surrounding water will play an important role in stabilizing OH adsorbates via hydrogen bonds.[38]

Additionally, it is also possible that thermal dissociation of water can result in the formation of OH groups on the surface. For this we considered the following reaction:

$$H_2O_{ads} \rightarrow OH_{ads} + H_{ads}. \tag{9}$$

This reaction has a ΔG of -0.23 eV on Pt(533), $+0.33$ eV on Pt(553), and $+0.47$ eV on Pt(111) at 298 K, again with all adsorbates binding to their most stable sites in complete isolation. The results suggest that on the step edge of Pt(553) reaction (9) is endothermic, while for the step edge of Pt(533) water has a thermodynamic tendency to dissociate. On Pt(111) reaction (9) will not take place without further stabilization of OH.

In conclusion, it can be assumed that in the low coverage limit on the Pt(533) surface, water will dissociate into H and OH on steps, depending on the barrier of the dissociation reaction, whereas on the Pt(553) surface there is no driving force towards forming OH.

CONCLUSIONS

In this paper, we presented the DFT-GGA adsorption energetics of water and the water-related fragments OH, O, and H on stepped Pt surfaces in the low coverage limit for comparison with experimental results on the same surface. The general trend indicates that the (100) step edge present in Pt(533) shows significantly enhanced binding for all studied species, while the (111)/(110) step edge present in Pt(553) shows no significant increase in binding energy for H, noticeable increases for O and OH, although less than the Pt(533) step edge, and similar increases for H$_2$O when compared to Pt(533). We would ascribe this stronger bonding of the (100) step to its more open character compared to the (111) step, though we note that there is no noticeable change in the local d-band center. Comparison of these results to experimental TPD measurements previously obtained in our group shows that the general trends of the low coverage results of the TPD measurements are matched by the calculations. Nevertheless, for the high coverage limit, as well as for water and OH, where interactions between the adsorbates play a large role, trends may no longer be explained with the present results. The benchmark study presented here gives confidence that including interactions between adsorbates and water should yield valuable results that will improve the theoretical description of realistic platinum surfaces.

[1]H. A. Gasteiger, S. S. Kocha, B. Sompalli, and F. T. Wagner, Appl. Catal. B **56**, 9 (2005).
[2]M. T. M. Koper, *Fuel Cell Catalysis: A Surface Science Approach* (Wiley, 2009).
[3]A. Rabis, P. Rodriguez, and T. J. Schmidt, ACS Catal. **2**, 864 (2012).
[4]N. M. Marković and P. N. Ross, Surf. Sci. Rep. **45**, 117 (2002).
[5]M. T. M. Koper, Nanoscale **3**, 2054 (2011).
[6]R. A. Olsen, S. C. Bădescu, S. C. Ying, and E. J. Baerends, J. Chem. Phys. **120**, 11852 (2004).
[7]R. Burch, S. Daniells, J. Breen, and P. Hu, J. Catal. **224**, 252 (2004).
[8]M. Rafti, J. L. Vicente, A. Albesa, A. Scheibe, and R. Imbihl, Surf. Sci. **606**, 12 (2012).
[9]L. Arnadottir, E. M. Stuve, and H. Jónsson, Surf. Sci. **604**, 1978 (2010).
[10]C. Buso-Rogero, E. Herrero, J. Bandlow, A. Comas-Vives, and T. Jacob, Phys. Chem. Chem. Phys. **15**, 18671 (2013).
[11]M. J. T. C. van der Niet, A. den Dunnen, L. B. F. Juurlink, and M. T. M. Koper, J. Chem. Phys. **132**, 174705 (2010).
[12]Y. Tison, K. Nielsen, D. J. Mowbray, L. Bech, C. Holse, F. Calle-Vallejo, K. Andersen, J. J. Mortensen, K. W. Jacobsen, and J. H. Nielsen, J. Phys. Chem. C **116**, 14350 (2012).
[13]G. Kresse and J. Hafner, Phys. Rev. B **47**, 558 (1993).
[14]G. Kresse and J. Hafner, Phys. Rev. B **49**, 14251 (1994).
[15]G. Kresse and J. Furthmueller, Comput. Mater. Sci. **6**, 15 (1996).
[16]G. Kresse and J. Furthmueller, Phys. Rev. B **54**, 11169 (1996).
[17]J. P. Perdew, K. Burke, and M. Ernzerhof, Phys. Rev. Lett. **77**, 3865 (1996).
[18]P. E. Blochl, Phys. Rev. B **50**, 17953 (1994).
[19]G. Kresse and D. Joubert, Phys. Rev. B **59**, 1758 (1999).
[20]D. R. Hamann, Phys. Rev. B **55**, R10157 (1997).
[21]H. J. Monkhorst and J. D. Pack, Phys. Rev. B **13**, 5188 (1976).
[22]M. W. Chase, Jr., C. A. Davies, J. R. Downey, Jr., D. J. Frurip, R. A. McDonald, and A. N. Syverud, J. Phys. Chem. Ref. Data **14**, Suppl. 1 (1985).
[23]J. I. Martínez, H. A. Hansen, J. Rossmeisl, and J. K. Nørskov, Phys. Rev. B **79**, 045120 (2009).
[24]F. Calle-Vallejo, J. I. Martnez, J. M. Garca-Lastra, M. Mogensen, and J. Rossmeisl, Angew. Chem., Int. Ed. **49**, 7699 (2010).
[25]D. Loffreda, Surf. Sci. **600**, 2103 (2006).
[26]See supplementary material at http://dx.doi.org/10.1063/1.4869749 for a full list of adsorption sites, their associated energies, vibrational frequencies, and additional geometry information.
[27]R. A. Olsen, G. J. Kroes, and E. J. Baerends, J. Chem. Phys. **111**, 11155 (1999).
[28]S. Gudmundsdóttir, E. Skúlason, and H. Jónsson, Phys. Rev. Lett. **108**, 156101 (2012).
[29]S. Gudmundsdóttir, E. Skúlason, K.-J. Weststrate, L. Juurlink, and H. Jónsson, Phys. Chem. Chem. Phys. **15**, 6323 (2013).
[30]G. Tritsaris, J. Greeley, J. Rossmeisl, and J. Nørskov, Catal. Lett. **141**, 909 (2011).
[31]T. Jacob, R. P. Muller, and W. A. Goddard, J. Phys. Chem. B **107**, 9465 (2003).
[32]P. J. Feibelman, S. Esch, and T. Michely, Phys. Rev. Lett. **77**, 2257 (1996).
[33]S. Meng, E. G. Wang, and S. Gao, Phys. Rev. B **69**, 195404 (2004).
[34]P. Vassilev, R. A. van Santen, and M. T. M. Koper, J. Chem. Phys. **122**, 054701 (2005).
[35]E. M. Karp, C. T. Campbell, F. Studt, F. Abild-Pedersen, and J. K. Nørskov, J. Phys. Chem. C **116**, 25772 (2012).
[36]V. Tripković, E. Skúlason, S. Siahrostami, J. K. Nørskov, and J. Rossmeisl, Electrochim. Acta **55**, 7975 (2010).
[37]M. J. T. C. van der Niet, N. Garcia-Araez, J. Hernández, J. M. Feliu, and M. T. M. Koper, Catal. Today **202**, 105 (2013).
[38]W. Lew, M. C. Crowe, C. T. Campbell, J. Carrasco, and A. Michaelides, J. Phys. Chem. C **115**, 23008 (2011).